
Embedded System Performance Analysis for Implementing a Portable Drowsiness Detection System for Drivers

Minjeong Kim¹, Jimin Koo²

¹ Monta Vista High School, Cupertino, CA 95014; minjeongsunnykim@gmail.com

² Cupertino High School, Cupertino, CA 95014; jimin.skoo@gmail.com

Abstract: Drowsiness on the road is a widespread problem with fatal consequences; thus, a multitude of solutions implementing machine learning techniques have been proposed by researchers. Among existing methods, Ghoddoosian et al.'s drowsiness detection method utilizes temporal blinking patterns to detect early signs of drowsiness. Although the method reported promising results, Ghoddoosian et al.'s algorithm was developed and tested only on a powerful desktop computer, which is not practical to apply in a moving vehicle setting. In this paper, we propose an embedded system that can process Ghoddoosian's drowsiness detection algorithm on a small mini-computer and interact with the user by phone; combined, the devices are powerful enough to run a web server and our drowsiness detection server. We used the AioRTC protocol on GitHub to conduct real-time transmission of video frames from the client to the server and evaluated the communication speed and processing times of the program on various platforms. Based on our results, we found that a Mini PC was most suitable for our proposed system. Furthermore, we proposed an algorithm that considers the importance of sensitivity over specificity, specifically regarding drowsiness detection algorithms. Our algorithm optimizes the threshold to adjust the false positive and false negative rates of the drowsiness detection models. We anticipate our proposed platform can help many researchers to advance their research on drowsiness detection solutions in embedded system settings.

Keywords: drowsiness detection; embedded systems, WebRTC, AioRTC, facial detection, blink detection

1. Introduction

1.1 Background

Drowsiness on the road is a widespread problem with fatal consequences. Each year, 1.35 million people are killed on roadways around the world, according to the World Health Organization's Global Status Report on Road Safety in 2018 [1]. 328,000 drowsy driving-related crashes occur annually in the United States alone, according to a study by the AAA Foundation for Traffic Safety [2]. Furthermore, NHTSA estimates suggest that fatigue-related crashes cost society \$109 billion each year, on top of property damage [2]. Studies from the National Sleep Foundation revealed that 50% of U.S. adult drivers admit to consistently driving while drowsy, and 40% admit to falling asleep behind the wheel at least once in their driving careers [3]. Thus, drowsy driving is a ubiquitous problem that claims heavy social and economic tolls. It must be promptly addressed in order to save irreplaceable human lives and economic damage.

1.2 Prior work

Existing work on this problem focuses on identifying explicit signs of drowsiness, which is less effective in detecting and alerting users because the reaction time between alerting and acting must be considered.

Feng You et al. [4] proposed a program that detects drowsiness by checking whether eyes are closed using eye aspect ratios calculated from detected facial landmarks. The program uses a deep-cascaded convolutional neural network to detect the face, then a `cv::lib` facial landmark detector to analyze the facial landmarks. Most of the research went into the development of the face detection model. The drowsiness detection is performed in real-time using a support vector machine (SVM) trained offline that predicts if the eyes are open or closed in a given frame. If the ratio of the number of closed-eye frames to the number of open-eyed frames is greater than a designated threshold, the driver is labeled`

as drowsy. However, due to the complexity of drowsiness, previous research [5] shows that the points behind a single frame or blink cannot determine the drowsiness of a person. Also, the algorithm cannot detect early signs of drowsiness if the driver's eyes are not closing periodically. When the number of closed-eye frames is significantly greater than the number of opened-eye frames, it may be too late to effectively prevent imminent car accidents.

Manishi et al. [6] proposed a method that also detects drowsiness by checking if the eyes are open or closed. The program uses a Viola-Jones algorithm to detect the eyes and mouth, from which a convolutional neural network is used to detect if the eyes and mouth are open or closed. Closed eyes or wide-open mouths indicate drowsiness. Using the NTHU Drowsy Driver Detection Dataset, this model takes into consideration the different situations that the user may use the program, such as in the dark and with or without glasses. Like Feng You et al. 's research, however, this approach can only detect severe drowsiness and not the early signs of drowsiness.

Lastly, Ghoddoosian et al. [7] proposed a drowsiness detection method that includes a dataset and a model that detects the early signs of drowsiness. The proposed LSTM model takes into consideration that early signs of drowsiness detection can be detected by a distinct sequence of blinking patterns such as the speech of eyes closing or opening, duration of the blinks, amplitude, and frequency. These temporal features of blinks resulted in accurate predictions. The method detects faces using Dlib's face detection model [8], and then uses Kazemi and Sullivan's [9] model to detect facial landmarks. Finally, it uses Soukupova and Cech [10] 's model to detect blinks. The LSTM model uses data on a sequence of blinks to classify a person's current state as alert, low-vigilant or drowsy. The LSTM model was trained on a dataset of 60 different individuals of a wide range of ages and six different ethnicities who provided videos of themselves in various states of drowsiness. This algorithm appeared the most promising because it could detect early signs of drowsiness, which is why we decided to use this model as a base model for our research. However, this method was developed on a powerful desktop computer, and further development is needed in order to implement it in a portable setting. The proposed model has not been optimized for an in-vehicle setting, and future research on how to optimize this model to trade-off between the convenience and safety of the driver is necessary.

1.3 Our approach

We propose a portable drowsiness detection system consists of a phone and a mini server which can be paired and placed in a car. The phone serves as the camera and touch-display, and the mini server which is plugged into the car's auxiliary power outlet runs the drowsiness detection model. The program runs in real time. We also propose a threshold finder and drowsiness value voting algorithm. We put our research efforts into the following two parts: developing a portable embedded system for performing drowsiness detection and developing an algorithm that finds the threshold for each model and votes for the final drowsiness value. For the drowsiness detection model, we used the same drowsiness detection model as proposed by Ghoddoosian et al. [7]. Our proposed approach not only considers the temporal aspect of drowsiness detection but also allows the model to be utilized in a real-time car setting.

1.3.1 Portable Embedded System

In this paper, we also propose the hardware/software implementation of a portable drowsiness detection system that can be used in the car. integrated the drowsiness model into a hardware setup. In the user's car, a powerful mini-PC server is set up, and the phone connects to the server and run the drowsiness detection web app. This approach also ensures privacy since the user's data stays in the mini server instead of being shared on the internet. In order to develop our system, quantitative analysis of the communication speed and of the performance of the system in a portable setup needs to be performed. The analysis allows us to decide which of the candidate hardware should be used for our proposed system. We tested the candidate systems and selected the device that can both

accommodate the complex AI performed for drowsiness detection and be conveniently placed in a car.

1.3.2 Threshold Optimization Algorithm and Voting Algorithm

Furthermore, we propose a method for optimizing the threshold for our model, which divides blink sequences into the categories: alert and drowsy. The drowsy category includes both the low vigilant and drowsy categories from Ghoddoosian et al.'s model. We hypothesize that on the road, our drowsiness detection model requires a trade-off between sensitivity and specificity. Sensitivity refers to the ability of the model to accurately detect drowsiness when the driver is drowsy, while specificity refers to the ability of the model to correctly detect alertness when the driver is not drowsy. We decided that the sensitivity of our model is much more important than specificity, as poor specificity causes inconvenience by falsely alerting the driver, but poor sensitivity can cause life-threatening problems. We believe that simply minimizing the difference between the ground truth labels and model predictions is not enough. We propose an algorithm that creates a trade-off between sensitivity and specificity. We also calculate the final drowsiness state prediction based on a voting method of multiple models that our program uses.

2. Materials

In this section, we describe the hardware configuration of our proposed embedded system that runs the drowsiness detection algorithm in real time, as well as the drowsiness detection algorithms, threshold optimization method, and the real-time voting algorithm to calculate the final drowsiness value. As shown in Figure 1, the client can be placed near the front of the car where the camera of the client can stably detect the driver's face. The

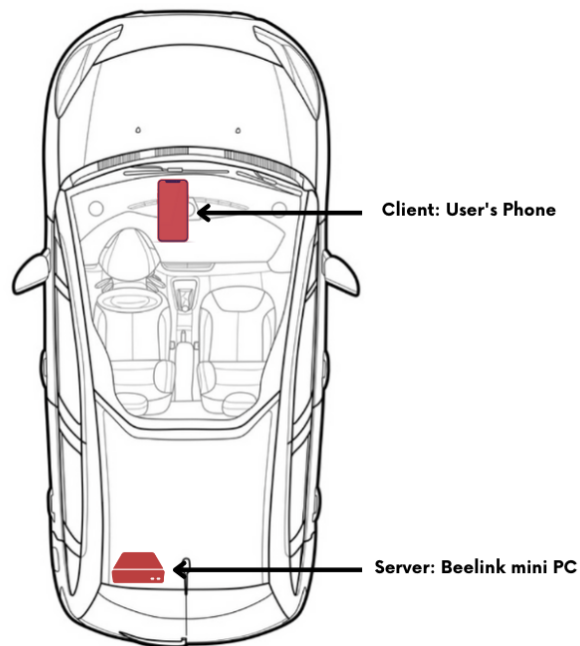


Figure 1. Car installation example of our proposed solution. The client is a phone that can be attached near the dashboard area. The front facing camera should see drivers face in order to detect blinks. The server can be positioned anywhere in the car as long as 12V power can be provided. The client and server is communicating wirelessly through Wi-Fi connection

server can be placed anywhere in the car. For example, it can be placed in the trunk and use the 2V power outlet as its source of power.

2.1 Hardware Setup

As described earlier, we are proposing using two parts to detect drowsiness: a client and a server. The client can be any mobile phone that has a camera and Wi-Fi capability. The phone should also have a web browser that can load our web app. Since the server runs the web server and drowsiness detection algorithm, it must have adequate communication performance and processing power. In this paper, we explain how we choose a device for the server.

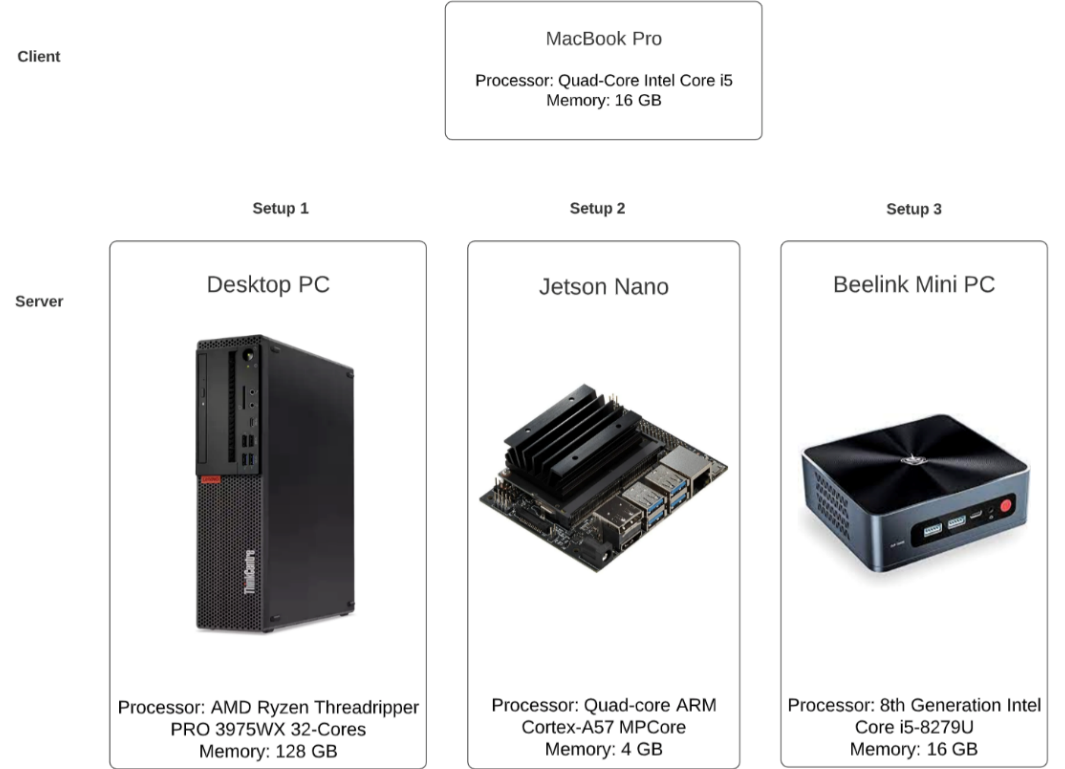


Figure 2. Setups we tested: Client stayed as the MacBook Pro, while the device supporting the varied across three platforms as shown above.

We tested our app on three different setups with varying devices running the server side of our app. The details for each of the devices used are shown in Figure 2. All three of the setups used the MacBook Pro to host the client side, which will be replaced by a phone in a car setting. For the server side, we tested a Windows 10 Computer, a Jetson Nano, and a Beelink Mini-computer and compared their performance of processing video frames and retrieving the data needed to make a drowsiness prediction. First, we used a Windows 10 PC to develop our web app and debug code. We used the communication throughput measured with this setup as a reference for the other servers. Then, we used the Jetson Nano and Beelink Mini PC, which is much smaller in size and thus suitable to be placed in a car.

2.2 Software

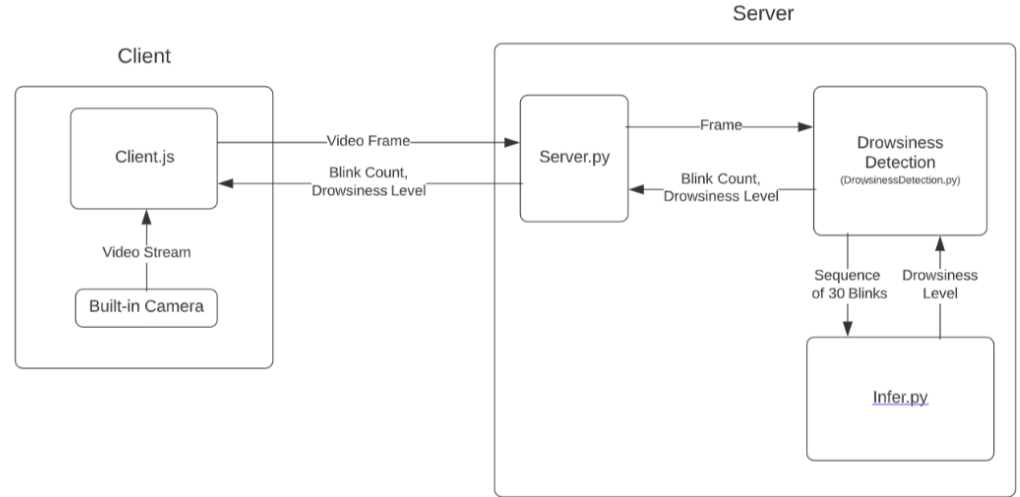


Figure 3. Proposed drowsiness detection SW architecture that runs the web app interface. Major block di-agrams are shown for the client and server side.

The overall architecture and block diagrams of our web app's software are shown in Figure 3. The software consists mainly of two parts: the client side and the server side.

2.2.1 Client

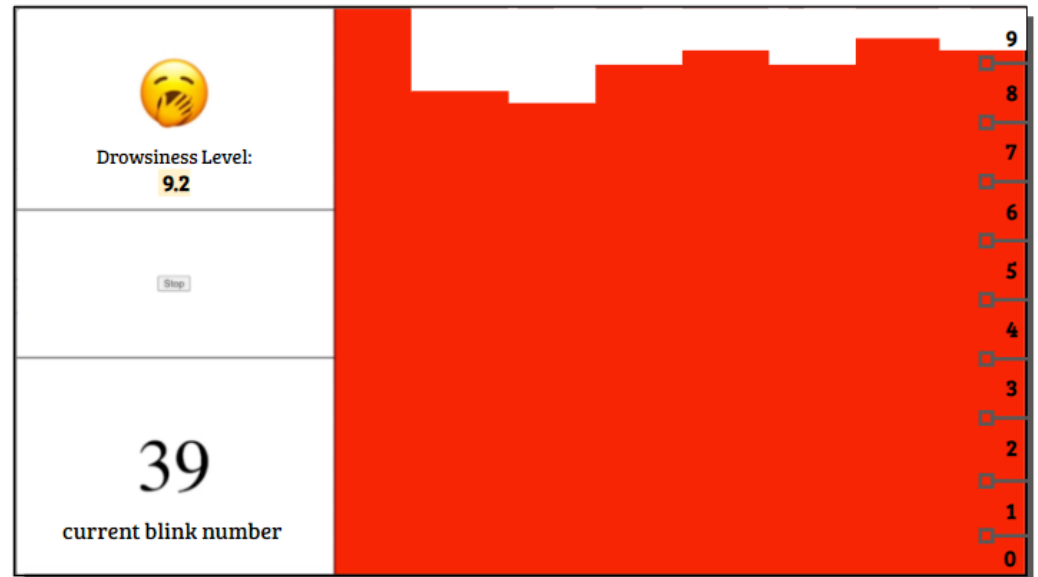


Figure 4. Running example of the user interface. The emoji on the top right describes the current drowsiness status and the bar chart displays the historical drowsiness value over time. On the bottom right, the number of detected blinks is shown so that users can know whether the algorithm is running without error.

Our system was built to be compatible with phones: the phone functions form the “client” part, utilizing the camera and screen to communicate with users, while the server functions form the computational device. When the client connects to the server, it automatically downloads the files needed to run the web app, which include index.html, client.js, and base.css. These files are provided in the AioRTC server example. Index.html provides the input interface to the user and displays the elements that users interact with as in **Figure 4**, while client.js includes the majority of the functionality of the web app, such as video display, WebRTC communication, display of the drowsiness detection level,

and history of the drowsiness levels in real-time. The CSS file contains the styling elements, which include color schemes and the formatting of the main page. Currently, we are using a simple method of alerting drivers by displaying their drowsiness value and changing the color of a bar graph to red when the user's drowsiness level passes a certain threshold.

2.2.2 Server

For our server, we utilized AioRTC (<https://github.com/aiortc/aiortc>), which is an open source library for Web Real-Time Communication (WebRTC) and Object Real-Time Communication (ORTC) in Python. We chose to use AioRTC because its implementation is simple and readable compared to Webrtc. In addition, our code handles a local server, meaning there is required communication between the client and the backend (models, server.py). Aiortc was most suitable because it can send data from the 'client' to the 'server' without having to download data locally before analyzing it, ultimately reducing lag. When the device begins detecting drowsiness upon the driver's request, the client (Client.js) sends video frames to the Server.py. We modified server.py to include a section that sends and receives data from the drowsiness prediction server. First, the server sends a fixed 2D array of the video frame to the drowsiness prediction file, DrowsinessDetection.py. DrowsinessDetection.py uses the RNN drowsiness detection model to predict and return drowsiness values along with the total number of collected blinks to server.py. The client receives the information and displays it on the HTML page. We explain DrowsinessDetection.py in more detail in section 2.3.1.

2.3 Drowsiness Detection Model

In the following sections, we summarize the algorithms used and developed by Ghoddoosian et al. for the drowsiness detection model, as well as our implementation that enables our proposed program to monitor the driver in real-time. We utilized Ghoddoosian et al.'s blink detection and feature extraction algorithms and offline training process making minimal changes to the code. For the live monitoring step, we modified the blink feature extraction code to include a function that sends data and receives a drowsiness value. This process is further explained in section 2.3.3. Furthermore, we developed a Threshold optimization algorithm and Voting Algorithm, which both serve to calculate the final real-time drowsiness prediction.

2.3.1 Blink Detection and Blink Feature Extraction

For our blink detection and blink feature extraction steps, we used the models proposed in Ghoddoosian et al.'s paper. We cloned their source code published in Github and combined it with the AioRTC webserver example. Their blink detection process can be divided into three steps: face detection, facial landmark detection, and blink detection. First, the program uses Dlib's pre-trained face detector, which is based on the standard Histogram of Oriented Gradients + Linear SVM method for object detection [8]. Ghoddoosian et al. then used Kazemi and Sullivan's [9] facial landmark detector because it was trained with an "in-the-wild dataset" which included videos filmed in various conditions (illuminations, facial expressions, head positions, rotations, etc.), thus making the model robust to a variety of environmental conditions [7]. For the blink detection step, Ghoddoosian et al. used Soukupova and Cech [10]'s blink detection model to perform the first blink detection step. Once a blink is detected, the blink retrieval algorithm uses the eye aspect ratios of the eyes to extract four features of the blink: amplitude, velocity, frequency, and duration. For further explanation of these values and their formulas, we refer readers to [7]. Each of these features is then normalized for each individual according to one-third of the blink features extracted from their alert video. This step is significant for this model as all the data are trained together, so differences across each individual's blinking pattern must be accounted for.

2.3.2 Offline Training and Threshold Optimization Algorithm

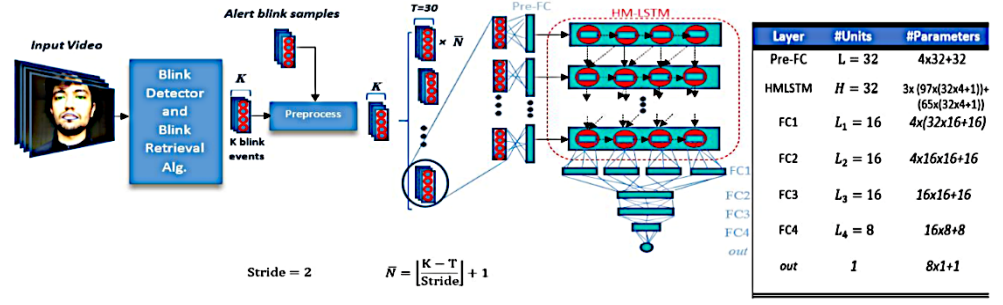


Figure 5. Drowsiness detection algorithm suggested in [7]

Regarding the drowsiness detection model, we used the model proposed by Ghodoosian et al. The structure of the model is shown in **Figure 5** from [7]. Ghodoosian et al. introduced an HM-LSTM network to incorporate the temporal element of drowsiness detection, since the Hidden Markov Model (HMM) from [11] indicates that expressions of drowsiness follow a temporal pattern. The model was trained on a dataset of 30 hours of RGB videos of 60 participants recording themselves in three drowsiness states alert, low-vigilant, and drowsy [7]. After the blinks of each of these videos are analyzed according to the algorithm explained in the previous section, the values are normalized and passed in as input for the HM-LSTM model. For details on the dataset with which the model was trained and the features of this HM-LSTM network, we refer readers to [7].

In Ghodoosian et al's paper, training.py trains the model by classifying each blink sequence's predicted drowsiness value, a number from 0.0 to 10.0, into three categories: alert, low-vigilance, and drowsy. Then, it compares the predicted category of blinks to the label of these blinks. The blinks are classified according to the ranges listed below.

- Alert: 0.0 predicted value < 3.3
- Low vigilance: 3.3 predicted value < 6.6
- Drowsy: 6.6 < predicted value 10.0

For our proposed solution for drowsiness detection for drivers, we added an additional step after the model training. First, we group the low-vigilance and drowsy categories together since we want to alert the driver once they begin expressing any signs of drowsiness. Also, we do not fix the threshold to one value (i.e. 3.33) as Ghodoosian's training algorithm does. Instead, we developed a customized threshold value which is determined by the ratio of false positive to false negative values of each model's confusion matrix. False negative (FN) rates indicate the fraction of predictions that incorrectly predicted a blink sequence as drowsy, while false positive (FP) rates indicate the fraction of predictions that incorrectly predicted a blink sequence as not drowsy. Both cases negatively impact the user experience, but we believe that decreasing the false negative rate is more important than lowering the false positive rate because safety is more important than convenience. We intentionally alter the threshold to perform the trade-off between the values. These rates change according to the threshold since the threshold determines whether a blink is predicted as drowsy or not drowsy. The process of finding the optimal threshold value will be explained in Methods Section 3.3. To test our optimization algorithm, we used the same dataset as the one used by Ghodoosian et al.

2.3.3 Online Monitoring and Voting Algorithm

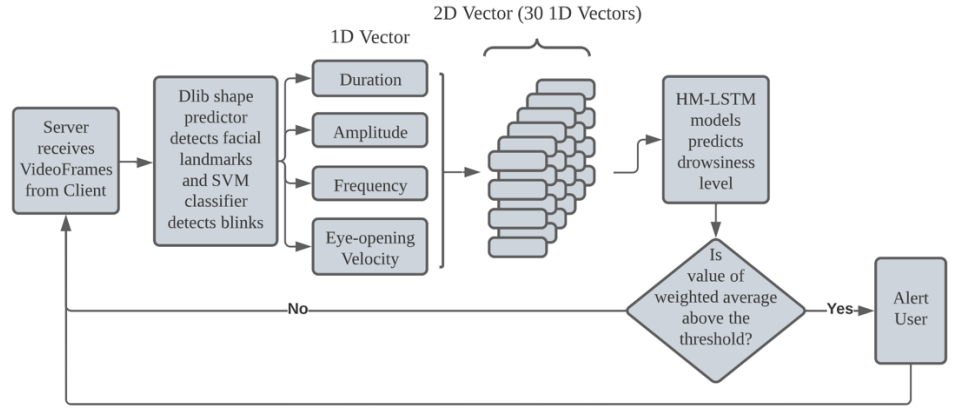


Figure 6. Real-time drowsiness detection and alert algorithm running in server

The general structure of the online monitoring step is shown in Figure 6. The HM-LSTM model proposed in [7] classifies 10-minute videos into various drowsiness states. However, for our approach, we developed an online monitoring algorithm that predicts the user's drowsiness level in the driver in real-time. The online monitoring algorithm is implemented in two main files: DrowsinessDetection.py and Infer.py. DrowsinessDetection.py returns the drowsiness value and number of blinks collected to the Aiortc server file, as mentioned in section 2.2.2. We developed DrowsinessDetection.py based on the blinkvideo.py, in which Ghoddosian et al.'s model is used to extract blink features for the model input. Instead of saving the blink features as a text file, however, DrowsinessDetection.py calls a function in Infer.py using a list of these values as the parameter. Infer.py then uses Tensorflow to run a session for each of the drowsiness detection models. Notably, because of the cross-validation step of the training method, there are five different drowsiness detection models trained with varying combinations of datasets. For further explanation of these models, we refer readers to [7]. Using the list of values of the input, each model outputs a drowsiness prediction, which is categorized according to the thresholds found by the Threshold Optimization Algorithm. Alert blink sequences are assigned the value 0.0, and drowsy blink sequences are assigned the value 10.0.

To obtain the final drowsiness value from the various values predicted by the multiple models generated during the cross-validation step, we developed an algorithm that finds the final value from their weighted average. Each model is assigned a weight value V_i , which is the sum of the true negative rate of the model and double the true positive rate for model i . We assigned a greater coefficient to the true positive rate than the true negative rate because we value sensitivity over specificity as explained in the introduction.

$$V_i = 2TP_i + TN_i \quad (1)$$

We then take the sum, S , of all V_i across models. S will be used to normalize the weighted values, as shown below.

$$S = \sum_{i=1}^N V_i \quad (2)$$

Finally, we define the prediction value, P , as the final predicted drowsiness value as shown below.

$$P = \sum_{i=1}^N \frac{V_i}{S} b_i \quad (3)$$

b_i is the binary value indicating whether the driver is drowsy or alert (1 if drowsy, 0 otherwise). If the value P surpasses 0.5, we predict the driver is drowsy, and the device alerts the user. The value P is displayed on the client's screen in the form of a bar chart, as illustrated in **Figure 4**.

3. Methods

We proposed a portable embedded solution for a drowsiness detection system that can be mounted on a car. In order to validate our solution, we decided to check the following characteristics: communication throughput between the client (the phone) and the server (the computer), processing speed to detect the face, facial landmarks, blinks, and drowsiness, and the optimized threshold value that considers the false positive and false negative rates of the drowsiness detection model. In the following sections, we describe the algorithms and environmental settings we developed to validate the system for each of the items above.

3.1 Communication Speed

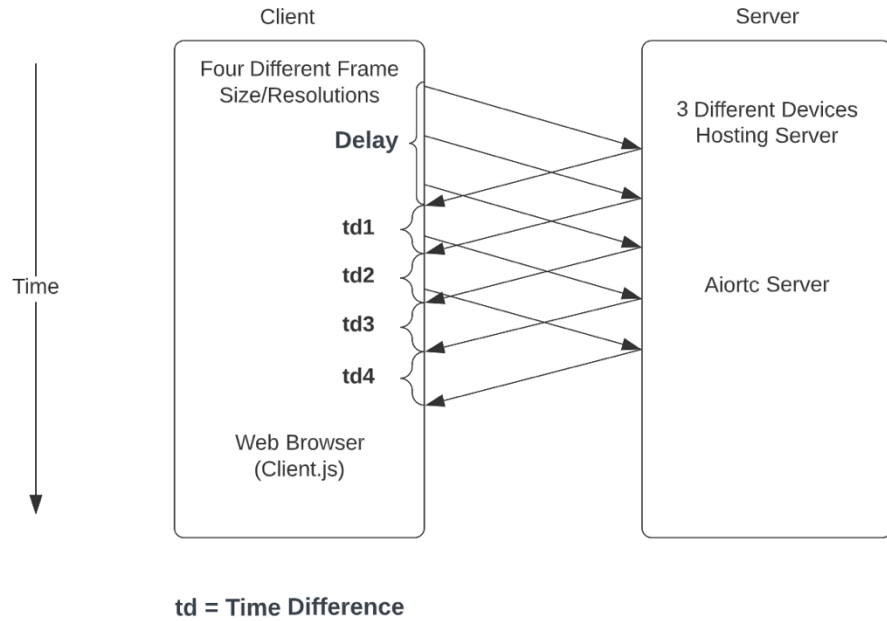


Figure 7. Method for measuring communication speed between client and server. The delay time is defined as the time for a video frame to sent to server and received back to client. The through is defined as the number frames that can be transferred per one second. We inserted a code to check the arrival time of the frames and measured the time difference between frames to measure the throughput.

In our proposed system, we divided the drowsiness detection into the server and client. Our system requires an adequately fast communication speed for the drowsiness system to work properly. If the speed is not fast enough to support the video frame rate, the frames that need to be sent from the client start to accumulate in the client, causing delays and eventually a memory overflow and system crash.

Communication speed can be described in terms of delay and throughput. Communication throughput determines the amount of data that can be sent in a second. In our case, we used frames per second (fps). The delay between the client and server determines the amount of time it takes for a frame sent from the client to be accessed by the server. In **Figure 7**, the time differences (td1, td2, td3, td4) represent the inverse of throughput while the Delay represents the communication delay. In our implementation, frames must be sent to the server at a rate equal to the that of camera in order for the system to properly function in real-time. On the other hand, the communication delay does not affect the

functionality of our system, and does not affect the total delay time of our system. Thus, we analyzed the only throughput of our system.

To evaluate the communication throughput of our proposed system, we used an open-source code in GitHub called AioRTC, which is a protocol that sends/receives multimedia data through WebRTC in real time. The code includes an example called "server", which lets users access the server via web browser and send and receive video images from the client. In the server example, the client sends video frames to the server, and the server processes the video (simple pass, edge detection, rotation, cartoon filter) and returns the processed video back to the client. We modified the client-side code to record the time when the client receives the returned frame from the server. For convenience, we also modified the code to configure the server to simply pass the video frame back to the client by default without modifying it.

To calculate the throughput, we first recorded the time difference between frames received by the client from the server. We expect the difference to be 33 ms since the video is recorded in 30 fps setting. If the communication speed between client and server is not fast enough, we expect the time to be larger than 33 ms.

We measured the communication throughput of our system in three different servers, as described in the materials section. Also, for each of the devices, we ran the program with four different image resolutions: 320x240, 640x680, 960x540, and 1280x720. Video resolution could affect the time it takes to send a video frame because of the increasing number of pixels, which could lead to a difference in time that is greater than the estimated 33.33ms period. For each of the device and resolution combinations (per resolution and per server type), we collected 500 data points and calculated the mean and standard deviation.

3.2 Processing Time

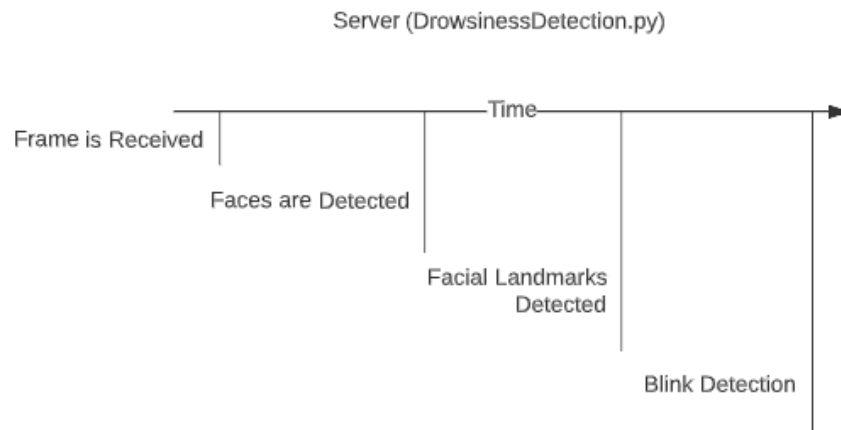


Figure 8. The timestamps which were used to analyze the processing time of drowsiness detection algorithm: the time required to detect face, detect facial landmarks, detect blinks are logged

In order to implement a drowsiness detection system in an embedded system for a vehicle, we needed to make sure the server is capable of processing the algorithm in real time. For a video with a frame rate of 30fps, the processing needs to be finished within a 33ms period. We ran the full drowsiness detection software, which includes the AioRTC server and drowsiness detection algorithm in our candidate platforms: Desktop PC, Jetson Nano, and Mini PC. The drowsiness detection algorithms that are time-sensitive in processing are the algorithms that need to process every frame. The following are important processes: face detection (Dlib), landmark detection (68-point landmark, OpenCV), and

blink detection (SVM classifier explained in [10]). The general flow of these processes is shown in Figure 8.

We measured the processing time for each algorithm by implementing logging code that records the following time stamps:

1. When the frame is received in the drowsiness detection algorithm
2. When the face is detected
3. When the 68 landmarks are detected
4. When blink detection is performed

By finding differences between these logged timestamps, we calculated the net processing time for each operation. In order to compare the processing time in the candidate platforms, we measured the timing using the following conditions:

- Devices: Desktop PC, Jetson Nano, Mini PC
- Resolutions: 320x240, 640x680, 960x540, and 1280x720

For each measurement, 450 data points were collected and the mean and STDev values were calculated. The drowsiness detection algorithm (Ghoddosian) which receives blink information and output drowsiness level is only performed when a blink is detected. This typically happens very slowly (every few seconds) compared to camera frame rate and thus not included in the processing time measurement procedure.

3.3 Threshold Optimization Algorithm

We propose a method to optimize the threshold value by sweeping through various threshold values and calculating the false positive and false negative rates for each. Since Ghoddosian et al., used a threshold value of 3.33 to divide the drowsy and low vigilant blinks, we sweep our threshold from 3.33 to 10 in increments of about 0.33. To evaluate the FP and FN of each threshold, we created a function that calculates the values of the confusion matrix given the threshold value, model, and dataset as input. From the confusion matrix, we get the FP and FN metrics, and calculate the value of $2FN + FP$. We plotted each of these values in a line graph to observe the general trend of these values according to the varying threshold. Ultimately, the algorithm searches for the threshold that outputs the minimum $2FN + FP$ value. In the formula below, we label f as the optimal threshold value.

$$\tilde{\theta} = \underset{\theta}{\operatorname{argmin}}\{2FN(\theta) + FP(\theta)\}, \quad (4)$$

where FN refers to False Negative Rate and FP refers to False Positive Rate. Ghoddosian et al. divide their dataset into five folds, resulting in five different drowsiness detection models created in the cross-validation step. We calculated the optimal threshold values for each of these models.

4. Results and Discussion

This section may be divided by subheadings. It should provide a concise and precise description of the experimental results, their interpretation, as well as the experimental conclusions that can be drawn.

4.1 Communication Speed

As shown in Figure 9, the median time difference between frames was consistently less than 33ms for all three cases: the computers, Jetson Nano, and NUC. It means there was no observable lag that accumulated with sending frames at each resolution. Time differences varied from a minimum of about 29ms to a maximum of up to 35ms, displaying a range of around 6ms. **Table 1** shows the average and standard deviation of all time differences across all devices and resolutions. The average of all time differences between frames is 33.30ms. As for the standard deviations, the average is 4.154ms across all devices

and resolutions. This standard deviation results from fluctuations of transfer time and frame processing time rather than frame capturing time variance in the camera.

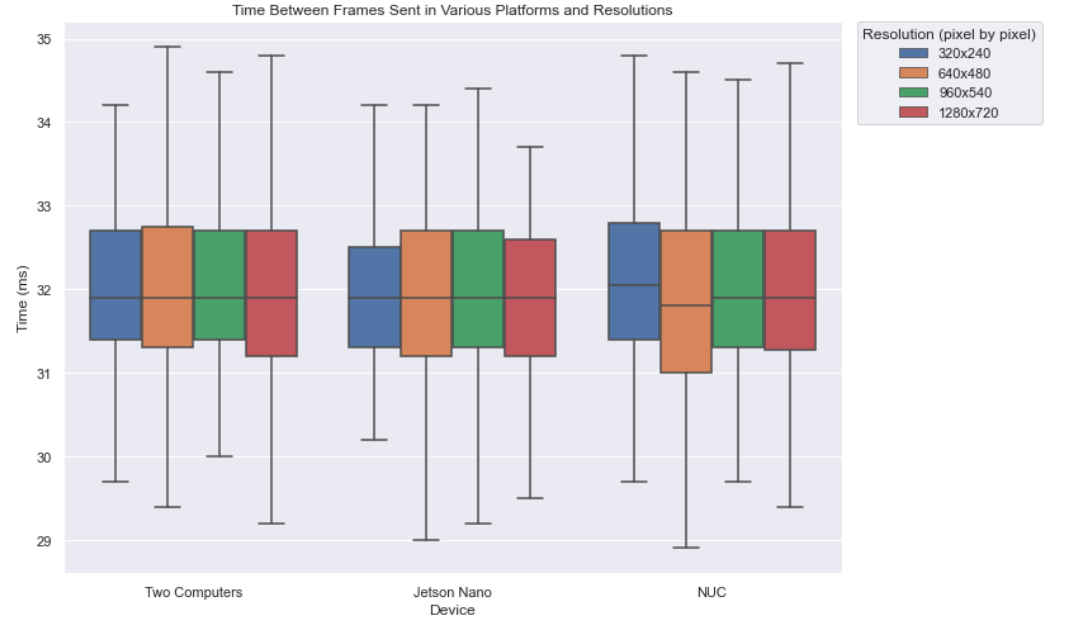


Figure 9. The time intervals between frames when a video stream is sent from client to server and then received back. Different video frame resolution did not affect the interval time. Regardless of the server platforms, there were variations in the values (± 4 ms) from the mean value between frames

Table 1. The time intervals between frames when a video stream is sent from client to server and then received back. Ideally the value of interval should match the frame rate of the video. The server was changed between desktop PC, Jetson Nano, and Mini-computer.

Video resolution	Desktop PC (ms)	Jetson Nano (ms)	Mini-computer (ms)
320x240	33.319 ± 3.892	33.326 ± 4.197	33.333 ± 3.930
640x480	33.255 ± 4.121	33.186 ± 5.255	33.320 ± 4.462
960x540	33.303 ± 3.722	33.299 ± 4.108	33.315 ± 3.932
1280x720	33.322 ± 3.984	33.303 ± 3.933	33.316 ± 3.867

In regard to communication speed, there were no apparent issues with throughput or delay across all platforms with a camera running at 30 fps. The communication speed is affected by the Wi-Fi performance of the devices in the client and server, wireless link quality, and the video frame processing time in client and server. Given that the wireless link will be within the area of a car and modern cellular phones support high speed Wi-Fi such as 802.11G/N/AC, we don't expect a shortage of speed. Furthermore, the video processing power in recent mobile phones and computers are fast enough to handle the transmission. We expected our solution to work in our proposed embedded system, which we validated through this experiment.

4.2. Processing Time

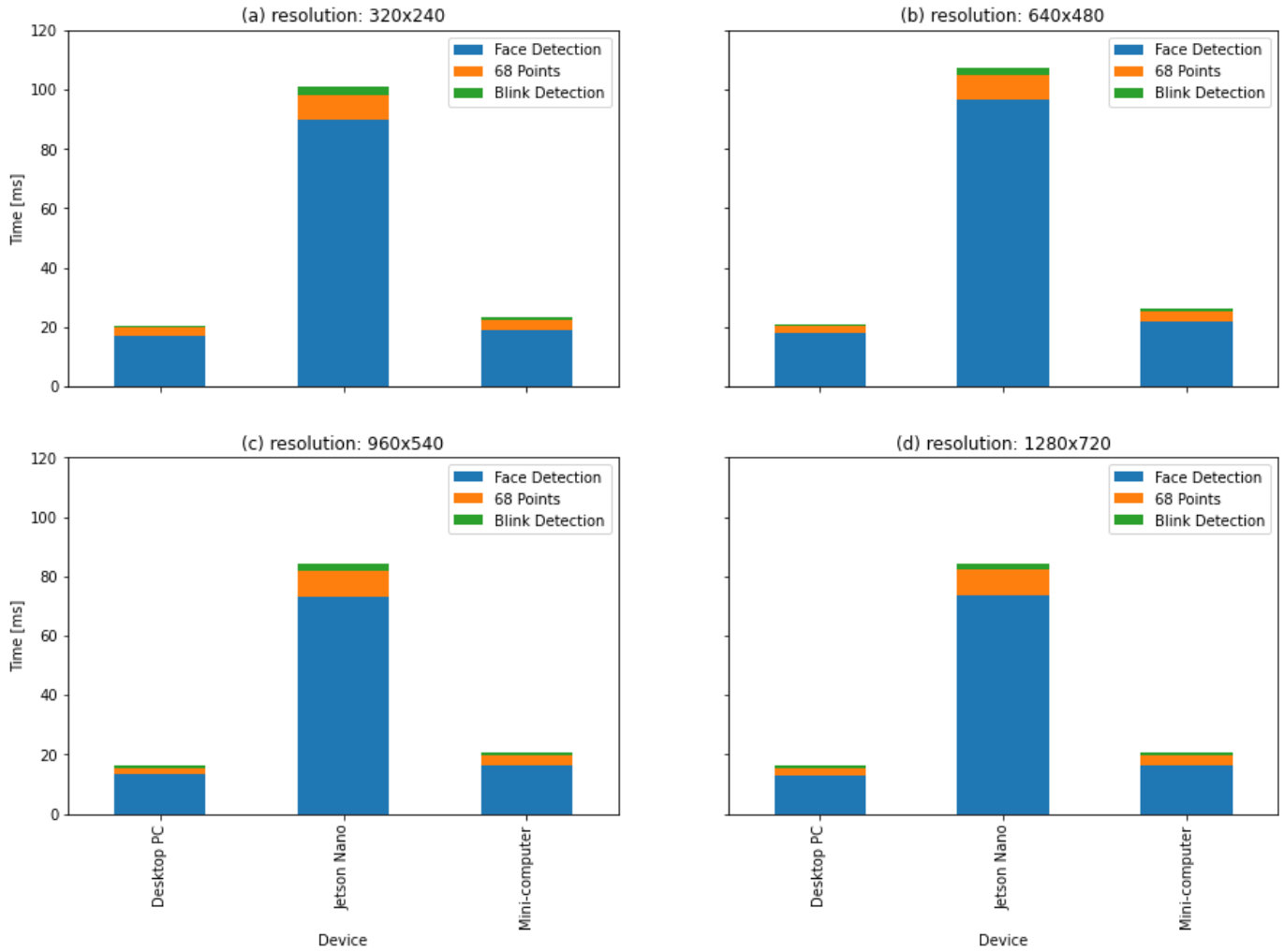


Figure 10. Inference time duration at various video resolutions. Across all of video resolutions the Jetson Nano take x4 more time than Desktop PC or mini-computer

Figure 10 shows the various processing times of detecting the face, facial landmarks, and blinks at various video resolutions and candidate platforms. Across all of the video resolutions, the Jetson Nano typically took 4 times more time than the Desktop PC or Mini-computer. The same data is shown in **Table 2**. Inference time duration of face detection, landmark detection, blink detection, and total. Desktop PC and mini-computer shows similar performance while at Jetson Nano the processing time is longer. units are in milliseconds, with the average processing time for each processing step and device displayed as well. In general, the average total processing time for the Windows 10 computer (Desktop PC) across all resolutions was 18.54s, with an average standard deviation of 0.85s. The average total processing time for the Jetson Nano was 94.27s, with an average standard deviation of 3.02s. Lastly, the average total processing time for the Beelink (Mini-computer) was 22.73, with an average standard deviation of 1.56s.

As demonstrated by the data mentioned above, the Jetson Nano Computer took significantly longer in running the inference operations at each frame when compared to other platforms. Even with the fastest operation time in Jetson Nano, in the case of 950x540 resolution, it took 84ms to process one frame, which far exceeds the desirable 33ms value for the 30fps camera video frame rate. Thus, Jetson Nano is an impractical device for drowsiness detection because the operation time that is longer than frame rate will accumulate lag over the time, making it impossible to alert drivers in real time. The Windows 10 computer performed inference operations in the shortest amount of time, but the size of the computer and the required power to run the computer makes it impractical for use

in cars. In the case of Mini-computers, the operation time meets the frame rate requirement. Even the longest operation time only took 26.364ms which was less than 33ms. The small size of the Mini-computer and efficient power consumption makes it possible to conveniently apply this system in cars. Therefore, we concluded that the Mini-computer is best suited to run our inference operation, which includes Face Detection, Landmark Detection, and Blink Detection.

Table 2. Inference time duration of face detection, landmark detection, blink detection, and total. Desktop PC and mini-computer shows similar performance while at Jetson Nano the processing time is longer. units are in milliseconds

Inference	Video Resolution	Desktop PC (ms)	Jetson Nano (ms)	Mini-computer (ms)
Face Detection	320x240	17.177 \pm 0.816	89.799 \pm 1.064	19.031 \pm 1.368
	640x480	17.752 \pm 0.925	6.453 \pm 2.048	21.935 \pm 1.928
	960x540	13.165 \pm 0.762	73.182 \pm 2.282	16.078 \pm 1.169
	1280x720	13.082 \pm 0.571	73.585 \pm 2.288	16.218 \pm 1.152
Landmark Detection	320x240	2.543 \pm 0.121	8.533 \pm 0.348	3.410 \pm 0.332
	640x480	2.570 \pm 0.283	8.633 \pm 0.590	3.346 \pm 0.651
	960x540	2.391 \pm 0.116	8.503 \pm 0.314	3.375 \pm 0.369
	1280x720	2.319 \pm 0.320	8.528 \pm 0.221	3.362 \pm 0.383
Blink Detection	320x240	0.835 \pm 0.063	2.645 \pm 5.164	1.037 \pm 0.124
	640x480	0.803 \pm 0.065	2.408 \pm 0.106	1.083 \pm 0.170
	960x540	0.790 \pm 0.316	2.398 \pm 0.108	1.019 \pm 0.128
	1280x720	0.745 \pm 0.037	2.401 \pm 0.069	1.035 \pm 0.125
Total	320x240	20.554 \pm 0.876	100.997 \pm	23.478 \pm 1.533
	640x480	21.126 \pm 1.042	107.524 \pm	26.364 \pm 2.018
	960x540	16.345 \pm 0.817	84.083 \pm 2.344	20.471 \pm 1.306
	1280x720	16.146 \pm 0.671	84.514 \pm 2.305	20.615 \pm 1.366

4.3 Threshold Optimization

To decide the drowsiness threshold for alerting the driver, we graphed the averages of the false negative and false positive percentages received from each participant depending on the threshold values as shown in Figure 11.

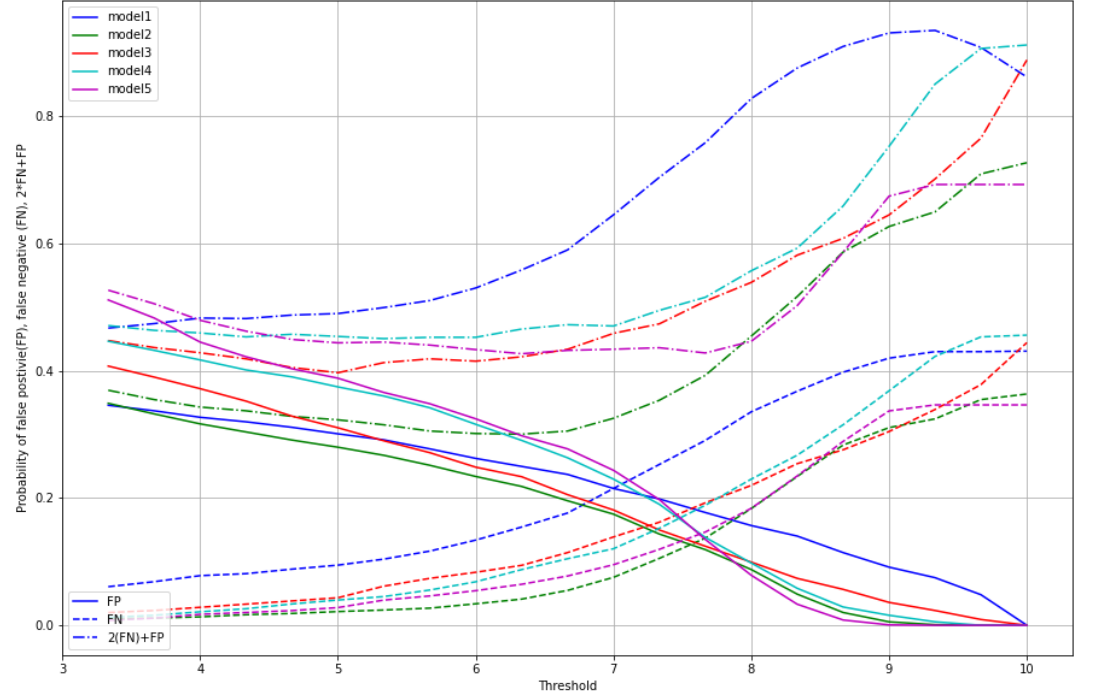


Figure 11. The false positive and false negative values are shown across a range of threshold values. Each color represents models differentiated by the trained data. The threshold needs to be determined by the trade-off between false positives and false negatives.

Table 3. The optimal threshold values for each model with minimum 2FN+FP

Model number	2FN+FP at Optimal Threshold	FP at Optimal Threshold	FN at Optimal Threshold	Optimal Threshold	2FN+FP at Default Threshold	FP at Default Threshold	FN at Default Threshold
1	0.47	0.35	0.061	3.33	0.59	0.24	0.177
2	0.3	0.22	0.041	6.33	0.31	0.20	0.054
3	0.4	0.31	0.043	5.00	0.43	0.21	0.114
4	0.45	0.36	0.055	5.33	0.47	0.26	0.104
5	0.43	0.30	0.064	6.33	0.43	0.28	0.077

As displayed in Figure 11, The FP rate tends to decrease as the threshold increases because a higher threshold leads to a greater confidence of drowsiness detection. Similarly, the FN rate tends to decrease as the threshold decreases because a lower threshold leads to a lower confidence in drowsiness detection. The values of 2FN + FP for most models experience a slight dip at relatively low thresholds before increasing at a fast rate. Table 3 summarizes the minimum values of 2FN+FP, FP, and FN at both the optimal threshold and default threshold, which is about 6.667 as explained in section 2.3.2. At the optimal thresholds, the minimum values of the 2FN+FP for each of the models range from 3.33 to 6.33. We can see that the FP values are higher and FN values are lower at the optimal threshold compared to the default threshold. The average FP value at the optimal threshold points was 0.31, and the average FN value was 0.053. Notably, the average FN rate is only about one-fifth of the FP rate. These values indicate that while the program may incorrectly alert the user about one third of the time, there is only a 5% chance that it will fail to detect drowsiness. This indicates that although drivers will almost always be alerted of their drowsiness, despite occasionally being annoyed by false alarms.

4.4 Future work

The dataset we used for our drowsiness detection algorithm was the one used by Ghoddoosian et al., which is composed of 10-minute recordings made by 60 people for each of the alert, low-vigilant, and drowsy states. We believe that since drowsiness behaviors differ from person to person, the decoding accuracy of the model can be greatly improved by personalizing the model for each user (training the model with a dataset consisting solely of the user's videos).

5. Conclusion

In this paper, we proposed an embedded system that allows a complex drowsiness detection model to be run in real-time. We found that by using Beelink Mini-computer as a server and phone as a web app client, the drowsiness detection algorithm can run smoothly with no accumulating lag time. Furthermore, we developed an algorithm that creates an optimal trade-off between the safety and the convenience of the user. We hope that other researchers aiming to convert their desktop algorithm into portable settings can extend our proposed methodology of validating the feasibility of implementing a portable system. Additionally, we hope that our drowsiness detection platform will be improved and researched further in a real-time automobile setting.

Acknowledgments: We would like to thank Mr. Jared Lera and the Applied Computing Foundation for providing guidance throughout our project and for suggesting Ghoddoosian's model as a foundation for our drowsiness detection system. Also, we would like to thank Professor Vassilis Athitsos from the University of Texas at Arlington for guiding us on the structure and submission process of this paper.

References

1. "Global status report on road safety 2018." <https://www.who.int/publications-detail-redirect/9789241565684> (accessed Sep. 11, 2022).
2. "Fatigued Driving - National Safety Council." <https://www.nsc.org/road/safety-topics/fatigued-driver> (accessed Sep. 11, 2022).
3. "About Half of Americans Admit to Driving While Drowsy," Pittsburgh Injury Law News, Dec. 18, 2019. <https://pittsburgh.legalexaminer.com/transportation/about-half-of-americans-admit-to-driving-while-drowsy/> (accessed Sep. 11, 2022).
4. F. You, X. Li, Y. Gong, H. Wang, and H. Li, "A Real-time Driving Drowsiness Detection Algorithm With Individual Differences Consideration," IEEE Access, vol. 7, pp. 179396–179408, 2019, doi: 10.1109/ACCESS.2019.2958667.
5. "Driver drowsiness detection through HMM based dynamic modeling | IEEE Conference Publication | IEEE Xplore." <https://ieeexplore.ieee.org/document/> (accessed Sep. 11, 2022).
6. "(PDF) Development of an Enhanced Drowsiness Detection Technique for Car Driver." https://www.researchgate.net/publication/344633633_Development_of_an_Enhanced_Drowsiness_Detection_Technique_for_Car_Driver (accessed Sep. 11, 2022).
7. R. Ghoddoosian, M. Galib, and V. Athitsos, "A Realistic Dataset and Baseline Temporal Model for Early Drowsiness Detection," ArXiv190407312 Cs, Apr. 2019, Accessed: Dec. 26, 2021. [Online]. Available: <http://arxiv.org/abs/1904.07312>
8. N. Dalal and B. Triggs, "Histograms of oriented gradients for human detection," in 2005 IEEE Computer Society Conference on Computer Vision and Pattern Recognition (CVPR'05), Jun. 2005, vol. 1, pp. 886–893 vol. 1. doi: 10.1109/CVPR.2005.177.
9. V. Kazemi and J. Sullivan, "One millisecond face alignment with an ensemble of regression trees," in 2014 IEEE Conference on Computer Vision and Pattern Recognition, Columbus, OH, Jun. 2014, pp. 1867–1874. doi: 10.1109/CVPR.2014.241.
10. T. Soukupova, "Real-Time Eye Blink Detection using Facial Landmarks," p. 8.
11. E. Tadesse, W. Sheng, and M. Liu. Driver drowsiness detection through hmm based dynamic modeling. In Robotics and Automation (ICRA), 2014 IEEE International Conference on, pages 4003–4008. IEEE, 2014.